Consensus between networks based on streamline fiber tracking and probabilistic fiber tractography

LI Qiaojun, JIANG Tianzi
Brainnetome Center, Institute of Automation, Chinese Academy of Sciences, Beijing 100190, P. R. China
E-mail: qjli@nlpr.ia.ac.cn

Abstract: Exploring structural brain network from diffusion MRI has been established as a useful method for understanding the topological organization of brain structure in health and disease. However, there is still no wildly accepted methods for constructing structural network. Definition of structural network edge is one of the most important issues in network construction. To generate network edges, streamline fiber tracking and probabilistic fiber tractography are wildly used. In this study, we explored the effect of networks based on these two different methods and investigated whether these two kinds of networks were mutually replaceable. To fulfill this, we compared four network properties (clustering coefficient, global efficiency, local efficiency, and shortest path length) between blind and sighted subjects. We found a high agreement in these properties between the two kinds of networks across a wide range of corresponding edge thresholds. Our findings demonstrated the utility of analyzing networks based on both these two methods to identify consensus results.

Key Words: structural network, streamline fiber tracking, probabilistic fiber tractography

1 Introduction

Exploring the topological organization of brain structure and their relation to neurological health and disease is very important for our understanding of human brain. Constructing the human structural network by diffusion MRI, which can describe the segregation and integration of human brain quantitatively in vivo, has gained a lot of attention [1]. Human brain network represented as a graph, is comprised of two vital elements, nodes representing a parcellation of the brain anatomy and edges representing white matter pathways connecting grey matter regions.

However, there is currently no wildly accepted method for constructing structural networks. A common method of defining nodes is to warp the structural image to an anatomical template. To date, many different templates, such as the AAL template and the Freesurfer template, have been used due to the absence of a well-defined template. Edges of human brain networks are also defined in many different ways. Among them, streamline fiber tracking and probabilistic fiber tractography are two wildly used methods. Streamline fiber tracking is a deterministic approach which give a single deterministic answer for the direction of the fiber [2]. Network based on this algorithm, herein called deterministic network, has been used to explore the differences between sighted and blind subjects [3], the relationship between brain network and intelligence [4] and many others. On the other hand, probabilistic fiber tractography is a probabilistic approach which depicts the variability of tractography results by estimating local fiber directions [4]. Network based on this algorithm, herein called probabilistic network, is also wildly used, for example, by Li et al. [5] and Parker et al. [6].

Studying the advantages and disadvantages of these two different methods on network construction as well as their relationship has been an important topic. However, no consensus conclusions have been reached, for example Buchanan et al. [7] thought that probabilistic networks were better for data analysis, while Bastiani et al. [8] suggested that deterministic networks were better for a preliminary study. In all these studies, the comparisons were fulfilled on the same dataset. However, the effect of these two kinds of networks for groups comparison, which is one of the most important way of network analysis, has never been studied.

In this study, we investigated the effects of the deterministic and probabilistic networks by applying to sighted subjects and blind subjects on four usually used global network properties. The high agreement between the four network properties demonstrated that networks analysis based on streamline fiber tracking and probabilistic fiber tractography are mutually replaceable for a preliminary study.

2 Materials and Methods

2.1 Subjects

97 right-handed blind subjects (68 males; mean age = 29.9 years, range 16-50 years) and 73 handedness-, age-, and gender-matched normal sighted controls (55 males, 18 females; mean age = 28.6 years, range 20-54 years) were recruited from the Special Education College of Beijing Union University or by advertisement in the local communities. All of these subjects have been carefully checked to ensure the subjects were suitable for this study with the following criteria: no history of any psychiatric or neurological illness, no drug or alcohol abuse, no contraindications to MR examination, right handed, and no different ages of onset of blindness in left and right eyes. This study was approved by the Ethics Committee of Tianjin Medical University, and an informed consent was signed by each participant before the study.

2.2 Data Acquisition and Preprocessing

All subjects were scanned using a 3.0 T Siemens MR scanner (Magnetom Trio, Siemens, Erlangen, Germany). The Integral Parallel Acquisition Technique was applied with an acceleration factor of 2 to reduce acquisition time and image distortion from susceptibility artifacts. Both diffusion tensor and T1-weighted 3D structural MR images were scanned. The protocol for DTI imaging were: repetition time/echo time (TR/TE) = 6000/90 ms; field of view (FOV) = 256 $\times$

This work is supported by the National Key Basic Research and Development Program (973) (Grant 2011CB707800).

256 mm^2; acquisition matrix = 128 $\times$ 128, reconstruction matrix = 256 $\times$ 256, in-plane resolution = 1 $\times$ 1 mm^2; 45 continuous axial slices, slice thickness = 3 mm; 30 diffusion gradients (b = 1000 s/mm^2) and one non-diffusion-weighted images (b = 0 s/mm^2). The acquisitions were repeated 2 times to improve the signal-to-noise ratio. The parameters for T1-weighted 3D images were: TR/TE = 2000/2.19 ms, inversion time = 900 ms, flip angle = 9°, slice thickness = 1 mm, FOV = 224 $\times$ 256 mm^2, 176 continuous sagittal slices, and voxel dimensions = 1 $\times$ 1 $\times$ 1 mm^3.

All T1-weighted and diffusion tensor MR images were checked by 2 radiologists to ensure each participant had high quality images. Analysis of the diffusion and structural MR images were performed using the software FSL 4.1 (http://www.fmrib.ox.ac.uk/fsl) including (1) correction for eddy current and head motion, (2) calculation of the diffusion tensor and fractional anisotropy (FA). After the above procedures, all T1-weighted images were co-registered to the b = 0 image of each individual using FLIRT (a toolkit in FSL) for getting a co-registered T1 image in DTI space for the following network construction.

2.3 Constructions of Anatomical Networks

2.3.1 Definition of Network Nodes

90 regions (45 for each hemisphere with the cerebellum excluded) from AAL template were used as the network nodes, which have been used in several previous studies [3, 4, 9]. Each individually co-registered T1 image was registered to the T1 template in Montreal Neurological Institute (MNI) space, and then the resulting inverse transformation was used to transform the AAL template in MNI space to DTI native space using FSL. After defining the nodes, we started to define edges to construct two different networks, deterministic network and probabilistic network.

2.3.2 Construction of Deterministic Network

Edges of the deterministic network were defined based on fibers from streamline fiber tracking method. It was constructed as follow using software Trackvis (including diffusion toolkit) and in-house scripts developed in the MATLAB 7.8 platform. Firstly, we employed the streamline fiber tracking method to compute the fibers of the entire brain for each subject. Only voxels with FA $>$ 0.3 in each region were chosen as seeds and the stop condition for tractography was voxels with an FA $<$ 0.15 or when the turning angle between adjacent voxels was greater than 45° [3]. Secondly, the number of fibers that started from an AAL region and ended in another AAL region was counted within each nodes pair of all the 90 nodes which formed a weighted network. Lastly, symmetric 90 $\times$ 90 binary anatomical networks were constructed for each subject by thresholding the weighted network with threshold value (TH_d) from 1 to 10.

2.3.3 Constructions of Probabilistic Network

Edges of the probabilistic network were defined based on probabilistic connectivity strength from probabilistic fiber tractography. It was constructed as follow using FSL and our in-house scripts developed in the Matlab 7.8 platform. Firstly, connectivity between nodes was estimated by performing probabilistic fiber tractography between each pair of the 90 AAL regions for each subject. We adopted the default settings in ProbTrack (a toolkit in FSL) for tractography. Secondly, connectivity strength between each pair of nodes was calculated. If the number of voxels in a seed region was n, the number of fibers passing through the target region divided by 5000 $\times$ n was then defined as the connectivity strength from the seed region to this target region. The connectivity strength between two nodes i and j was defined by averaging the strength from i to j and the strength from j to i. This definition for connectivity strength has been widely applied

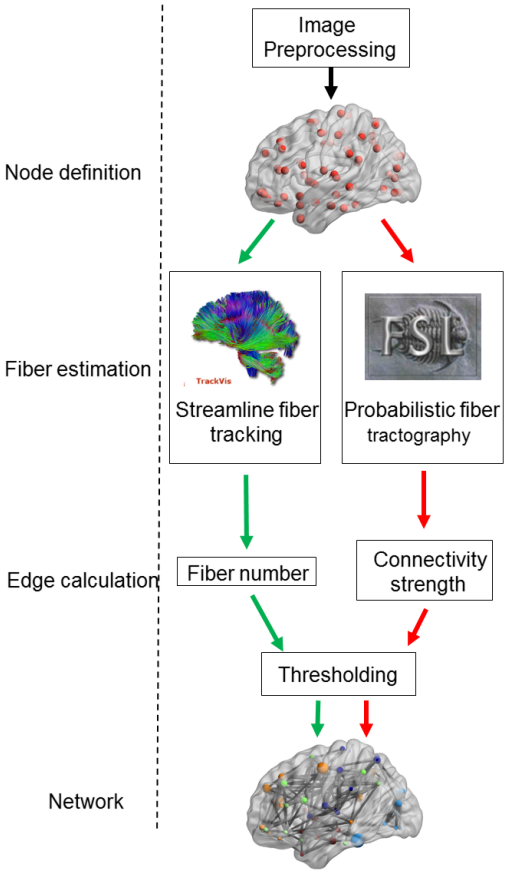

Fig. 1: Summary of construction of deterministic and probabilistic networks using structural and diffusion images. The pipeline stages are shown on the left and the implementations of the methods are shown on the right. Nodes were defined by registration of the cortical parcels in AAL atlas to diffusion space. Fiber density between all node pairs were then calculated by performing streamline fiber tracking (deterministic tractography) and probabilistic fiber tractography (probabilistic tractography). Edges for deterministic networks were defined by calculating the fiber number between node pairs and edges for probabiltistic networks were defined by calculating the connectivity strength. Lastly, edges with weighted-value were thresholded to generate binary networks for comparison of these two network construction pipelines. Note that both of two methods and the implementations used in this study had been used in many previous studies.

by previous studies [5, 10]. After above implementations, a weighted network was created for each subject. Lastly, symmetric 90 × 90 binary anatomical networks were constructed for each subject by thresholding the weighted networks with threshold value (TH_p) ranging from 0.01 and 0.1 at intervals of 0.005.

2.4 Properties of Anatomical Networks

Binary network is represented as an N × N (N = 90 in this study) graph, G, consisting of nodes (brain regions) and undirected edges (fibers or connectivity strength) between nodes. Here, we calculate some graph properties for network analysis.

Cost $Cost$ is usually used to evaluate the density of network and it is defined as the total edges of network divided the total edges when all nodes are full connected:

$$Cost = \frac{1}{N(N-1)} \sum_{i \in G} D_i,$$

where D_i, $i = 1, 2 \cdots, 90$ is defined as the number of direct edges to that node and G represents the network.

Clustering coefficient Clustering coefficient (C_p) quantifies the local efficiency of the network and is defined as

$$C_p = \frac{1}{N} \sum_{i \in G} C_i,$$

where

$$C_i = \frac{E_i}{D_i(D_i - 1)/2}$$

in which E_i is the number of edges among the node's direct neighbors.

Shortest path length Shortest path length L_p quantifies the global efficiency of the network and is calculated by

$$L_p = \frac{1}{N} \sum_{i \in G} L_i,$$

where

$$L_i = \frac{1}{N} \sum_{\substack{i \in G \\ i \neq j}} l_{i,j},$$

in which $l_{i,j}$ is the minimum number of edges for connecting the ith node to the jth node.

Global efficiency Global efficiency (E_{glob}) is a measure of the global efficiency of parallel information transfer in the network and is defined as

$$E_{glob} = \frac{1}{N(N-1)} \sum_{\substack{i \in G \\ i \neq j}} \frac{1}{l_{i,j}}$$

Local efficiency Local efficiency (E_{loc}) is a measure of the mean of local efficiency across all nodes in the network and is as

$$E_{loc} = \frac{1}{N} \sum_{i \in G} E_{i\_loc}$$

where

$$E_{i\_loc} = E_{glob}(G_i)$$

and G_i is defined as the set of nodes that are the direct neighbors of the node i.

2.5 Statistical Analysis

At the first, we calculated $Cost$, C_p, L_p, E_{glob}, and E_{loc} of deterministic and probabilistic networks from different TH_d and TH_p for all subjects using our in-house network analysis toolkit Brat (http://www.brainnetome.org/en/brat.html).

2.5.1 Networks Comparison Under the Same $Cost$ in sighted

By observing the range of $Cost$ value calculated above for deterministic and probabilistic networks. We chose a little $Cost$ values for our comparison. Then, we created the binary mean deterministic network with the $Cost$ value as follow: (1) Averaging all the deterministic networks of sighted subjects with that $Cost$, and (2) Binarizing the network by keeping the edges more than half of the subjects had. This procedure was replicated with a large $Cost$ value. With the same way, we created two binary mean probabilistic networks. Comparison was then done between the binary mean deterministic and probabilistic network under both little and large $Cost$ value.

2.5.2 Effect of Group Comparison between blind and sighted

Statistical comparisons of C_p, E_{glob}, E_{loc}, and L_p between blind and sighted groups were performed by using a two-sample two-tailed t-test for TH_d over a range of 1 to 10 and for TH_p from 0.01 to 0.1 at an interval of 0.005.

3 Results

3.1 Validation of the Deterministic and Probabilistic Networks

All sighted subjects were randomly divided into two groups for 100 times, one group with 36 subjects and the other 37 subjects. Independent two-sample two-tailed t-tests showed that no differences existed under $P < 0.05$ between the two groups in both deterministic and probabilistic networks. This means that comparison on C_p, E_{glob}, E_{loc}, and L_p will not cause false positive results.

3.2 Networks comparison under the same $Cost$ in sighted

To assess the relationship of deterministic and probabilistic networks, the $Cost$ value of the two kinds of networks for all TH_d from 1 to 10 and TH_p from 0.01 to 0.1 at an interval of 0.005 were calculated (Table 1). The two networks have nearly the same $Cost$ when TH_d = 1 and TH_p = 0.01, when TH_d = 2 and TH_p = 0.015, or when TH_d = 4 and TH_p = 0.02. What is more, high consistency between the values of the four calculated properties of the deterministic network and probabilistic network under the same $Cost$ were found (Fig. 3).

Additionally, binary mean deterministic and probabilistic networks with $Cost = 3$ and $Cost = 15$ were shown in Fig .2. Qualitatively, we observed that networks based on streamline fiber tracking would preserve more long-range connections, while networks based on probabilistic fiber tracking were more prone to reserve more short-range edges.

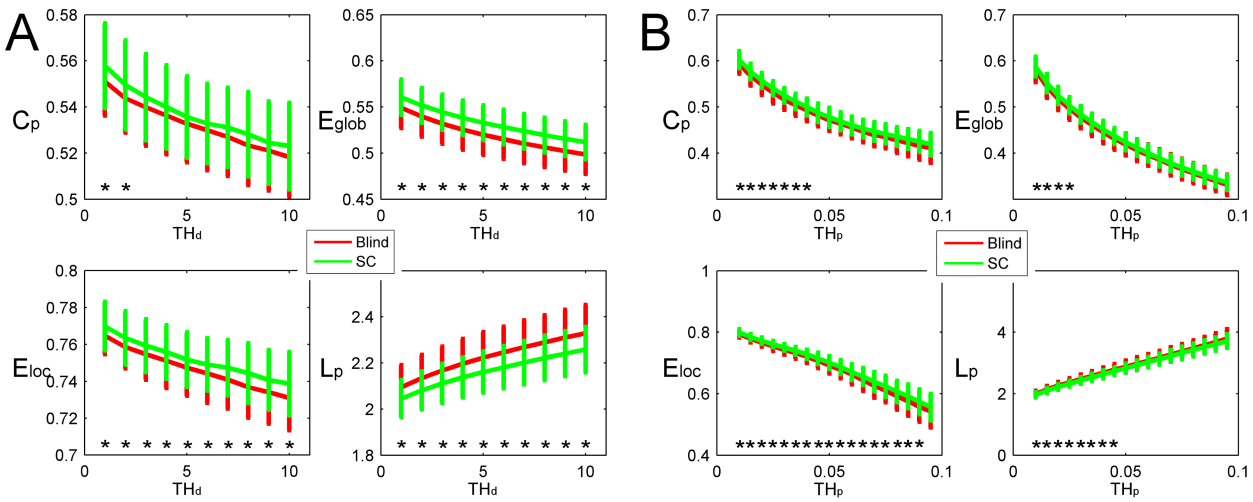

Fig. 3: Network properties (C_p, E_{glob}, E_{loc}, and L_p) of deterministic (A) and probabilistic networks (B) for blind and sighted groups. All these parameters are illustrated by the values (mean $\pm$ SD) of blind and sighted groups. Threshold values TH_d of deterministic network are in the range [1, 10] with increments of 1 and threshold values TH_p of probabilistic network are in the range [0.01, 0.1) with increments of 0.005. $\star$ demonstrated significant difference between blind and sighted groups with $P < 0.05$, uncorrected. Blindblind groupSC, sighted group.

Table 1: Cost value of deterministic and probabilistic networks based on different TH_d and TH_p. Only part are showed.

Deterministic Network		Probabilistic Network	
TH_d	Cost	TH_p	Cost
1	19.3	0.01	19.4
2	18.3	0.015	18.1
3	17.5	0.02	16.9
4	16.9	0.025	15.1
5	16.4	0.03	13.6
9	14.8	0.09	6.6
10	14.5	0.095	6.3

3.3 Comparison of Deterministic and Probabilistic Networks on Four Network Properties

For deterministic networks, the value of C_p, E_{glob}, and E_{loc} decreased and the value of L_p increased when the threshold TH_d increased from 1 to 10 (Fig. 3A). Also, for probabilistic networks, the value of C_p, E_{glob}, E_{loc}, and L_p showed the same trend as those for deterministic networks when the threshold TH_p increased from 0.01 to 0.1 (Fig. 3B). This trend existed for both sighted and blind groups.

The differences between sighted and blind were studied for all the TH_d and TH_p with $P < 0.05$. For deterministic networks, independent two-sample t-tests demonstrated that the blind group showed significant decreases in C_p when TH_d = 1 or 2, significant decreases in E_{glob} and E_{loc} when $TH_d \leqslant 10$, significant increases in L_p when $TH_d \leqslant 10$ compared with the sighted group; For probabilistic networks, independent two-sample t-tests demonstrated that the blind group showed significant decreases in C_p when $TH_p \leqslant 0.04$, significant decreases in E_{glob} when $TH_p \leqslant 0.025$, significant decreases in E_{loc} when $TH_p \leqslant 0.09$ and significant increases in L_p when $TH_p \leqslant 0.045$ compared with the sighted group.

4 Conclusions

In summary, this study explored the relationship of networks based on streamline fiber tracking method and networks based on probabilistic fiber tractography with a wide range of threshold values. By comparing the two networks on four different network properties, we found that networks based on streamline fiber tracking demonstrated the same effects as networks based on probabilistic fiber tractography for finding the differences between sighted and blind subjects. This finding suggested that we could adopt the network based on streamline fiber tracking to do preliminary network analysis considering that constructing networks based on probabilistic fiber tractography are time labored. More importantly, the findings imply the feasible of

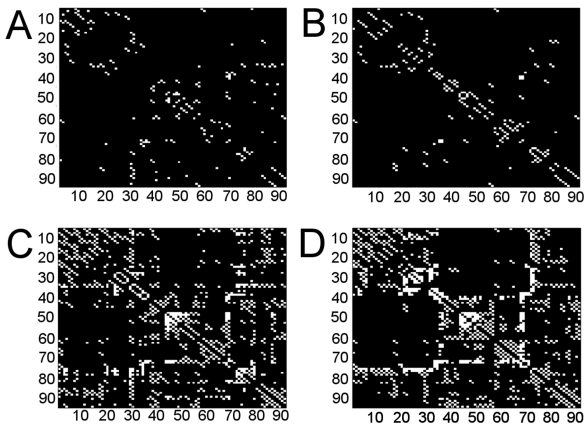

Fig. 2: Binary mean networks. (A) Binary mean deterministic network with $Cost = 3$. (B) Binary mean probabilistic network with $Cost = 3$. (C) Binary mean deterministic network with $Cost = 15$. (D) Binary mean probabilistic network with $Cost = 15$ Each figure shows a 90 $\times$ 90 square matrix, where the number in x and y axes correspond to the regions listed in AAL atlas, and white points in the squares dedicates the edges between pairs of brain regions.

analyzing networks based on both these two methods to identify consensus results.

References

[1] Sporns O, Tononi G, Kötter R. The human connectome: a structural description of the human brain. PLoS Comput Biol. 2005;1(4):e42.

[2] Mori S, Crain BJ, Chacko V, Van Zijl P. Three-dimensional tracking of axonal projections in the brain by magnetic resonance imaging. Annals of neurology. 1999;45(2):265–269.

[3] Li J, Liu Y, Qin W, Jiang J, Qiu Z, Xu J, et al. Age of onset of blindness affects brain anatomical networks constructed using diffusion tensor tractography. Cerebral Cortex. 2013;23(3):542–551.

[4] Li Y, Liu Y, Li J, Qin W, Li K, Yu C, et al. Brain anatomical network and intelligence. PLoS Comput Biol. 2009;5(5):e1000395.

[5] Li Y, Liu B, Hou B, Qin W, Wang D, Yu C, et al. Less efficient information transfer in Cys-allele carriers of DISC1: a brain network study based on diffusion MRI. Cerebral Cortex. 2012;p. bhs167.

[6] Parker CS, Deligianni F, Cardoso MJ, Daga P, Modat M, Dayan M, et al. Consensus between pipelines in structural brain networks. PloS one. 2014;9(10):e111262.

[7] Buchanan CR, Pernet CR, Gorgolewski KJ, Storkey AJ, Bastin ME. Test–retest reliability of structural brain networks from diffusion MRI. Neuroimage. 2014;86:231–243.

[8] Bastiani M, Shah NJ, Goebel R, Roebroeck A. Human cortical connectome reconstruction from diffusion weighted MRI: the effect of tractography algorithm. NeuroImage. 2012;62(3):1732–1749.

[9] Behrens T, Woolrich M, Jenkinson M, Johansen-Berg H, Nunes R, Clare S, et al. Characterization and propagation of uncertainty in diffusion-weighted MR imaging. Magnetic resonance in medicine. 2003;50(5):1077–1088.

[10] Johansen-Berg H, Behrens TE, Sillery E, Ciccarelli O, Thompson AJ, Smith SM, et al. Functional–anatomical validation and individual variation of diffusion tractography-based segmentation of the human thalamus. Cerebral cortex. 2005;15(1):31–39.